Automated Antenna Design Using Computational Intelligence and Numerical Optimization

Slawomir Koziel[1,2][0000-0002-9063-2647], Anna Pietrenko-Dabrowska[2][0000-0003-2319-6782], and Leifur Leifsson[3][0000-0001-5134-870X]

[1] Engineering Optimization & Modeling Center, Department of Engineering, Reykjavík University, Menntavegur 1, 102 Reykjavík, Iceland
koziel@ru.is

[2] Faculty of Electronics Telecommunications and Informatics, Gdansk University of Technology, Narutowicza 11/12, 80-233 Gdansk, Poland
anna.dabrowska@pg.edu.pl

[3] School of Aeronautics and Astronautics, Purdue University, West Lafayette, IN 47907, USA
leifur@purdue.edu

Abstract. Modern antenna design is a daunting task aimed at fulfilling diverse performance requirements and constraints imposed by specific application areas. Traditional techniques are heavily based on engineering experience. This limits the options considered for conventional architectures and leads to sub-optimal results. This study introduces an innovative approach to automated development of antennas. The introduced methodology incorporates computational intelligence techniques and numerical optimization procedures to carry out unsupervised antenna topology generation and fine-tuning its geometry parameters. The crucial component of the suggested method is a versatile parameterization involving elliptical-shaped patches and gaps, which can realize a massive variety of different shapes. Computational intelligence is used to execute a purely specification-driven antenna evolution process. The decision variables include a mixture of discrete and continuous parameters handled by a customized evolutionary algorithm (Stage I) and local optimizer (Stage II – fine tuning). The procedure is fully specification-based and requires no human-expert interaction whatsoever. The proposed framework has been comprehensively demonstrated by designing several devices of distinct characteristics (broadband, multi-band, compact). The findings underscore the versatility of the technique and its suitability to produce nonconventional structures with acceptable computational costs.

Keywords: Design automation, antenna systems, computational intelligence, optimization, unsupervised design.

1 Introduction

Antennas are vital building blocks of wireless communication systems, including mobile phones, satellite communications, radio-frequency identification, medical imaging, etc. Traditional design methods are typically based on the existing antenna topologies (e.g., available in the literature), which are modified to achieve the required functionality and performance. The process is iterative and involves trying out different

ICCS Camera Ready Version 2025
To cite this paper please use the final published version:
DOI: 10.1007/978-3-031-97557-8_26

architectural variations interleaved with parametric studies [1], or, recently, rigorous optimization, [2]. Optimization can be carried out in the local [3], global [4], [5], or multi-objective sense [6], [7]. The fundamental underlying tool is electromagnetic (EM) analysis. However, simulation-driven design is CPU intensive, which becomes a severe bottleneck when repetitive simulations are involved. Addressing this issue fostered the development of expedited methods, which include surrogate-assisted techniques [8], [9], machine learning (ML) routines [10], [11], response feature algorithms [12], or variable-resolution approaches [13]. A comprehensive review of metamodel-driven antenna design procedures is available in [14].

Boosting performance and realization of extra functionality is typically achieved by altering fundamental structures (e.g., patches, dipoles, etc.). The final product usually resembles the initial topology [15], while reaching it is laborious. This is highly restrictive regarding the number of alternative antenna geometries that may be investigated. Alternative methods include topology optimization (TO). It often involves spatial discretization and optimization-based assignment of individual cells (filled with metal or empty) [16], [17]. This approach is associated with the necessity of solving complex combinatorial tasks, even if only part of the antenna is discretized [18]. Another option is pixel antennas with a predefined arrangement of metal patches whose interconnections are decided upon through optimization [19], [20]. Free form TO is yet another technique [21], [22]. It offers significant flexibility but typically requires fast custom EM solvers to maintain acceptable computational expenses [23], [24]. Consequently, it cannot be integrated with commercial engineering design automation (EDA) tools. Also, it relies on gradient-based optimizers, which necessitates reasonable initial starting points to ensure the quality of the final structure.

This study outlines an innovative approach to the unsupervised design of antenna structures, which introduces several original contributions. The main focus is on ensuring flexibility, which is understood as a broad range of distinct geometries that can be generated and the capability of realizing diverse functionality (multi-band, wideband operation, etc.). Other prerequisites are integrality with commercial EM solvers and reasonable computational efficiency, which are critical from the practical engineering standpoint. Our methodology leverages versatile parameterization consisting of elliptical-shaped patches and gaps that can relocate within the substrate area and adjust their size to assemble antenna geometry through Boolean operations. Varying the number of building blocks and relocating them allows for the implementation of many topologies based on a restricted number of independent parameters. The design is entirely specification-based and utilizes computational intelligence to realize a global search stage (geometry evolution) and local optimization tools for final dimension tuning. The design problem is formulated to realize the assumed functionality and boost the antenna performance regarding the target operating frequency ranges and impedance matching level. The proposed approach has been demonstrated by designing several broadband and multi-band antennas of diverse characteristics, some experimentally validated for supplementary illustration. The obtained results corroborate the capability of the developed technique to produce high-performance unconventional antenna structures while ensuring computational efficiency. At the same time, the design process does not require any human-expert interaction. These findings underscore the framework's suitability for developing high-performance antennas for demanding applications in both academic and industrial settings.

ICCS Camera Ready Version 2025
To cite this paper please use the final published version:
DOI: 10.1007/978-3-031-97557-8_26

2 Antenna Design Using Computational Intelligence

This section explains the proposed unsupervised design framework. Section begins with discussing parameterization (Section 2.1), followed by a description of the computational model (Section 2.2) and the algorithms employed for antenna development in Section 2.3. The entire procedure is elucidated in Section 2.4.

2.1 Antenna Building Blocks

Geometry parameterization of the critical component of the presented framework. The prerequisites are as follows: (i) simplicity to ensure straightforward handling, (ii) flexibility to enable the construction of diverse topologies, (iii) a restricted number of decision variables to keep the underlying optimization task computationally tractable. The antenna parameters should include continuous ones, allowing for local tuning and discrete (to control the architecture's complexity). The components of the assumed parameterization are presented in Fig. 1. For illustration, a rectangular substrate is taken along with a rectangular ground plane. The antenna is excited through a relocatable discrete port. The front-side metallization is composed using N_P elliptical patches and N_G of gaps. These numbers may be fixed or treated as design variables. The positions and dimensions of all building blocks are relative to the substrate width W and length L. All parameters are aggregated into a vector $\boldsymbol{x}$. Figure 2 shows some randomly generated geometries demonstrating the flexibility of the discussed parameterization even when using a limited number of patches and gaps ($N_P = 5$ and $N_G = 3$). The antenna size can be optimized or fixed depending on the intended application.

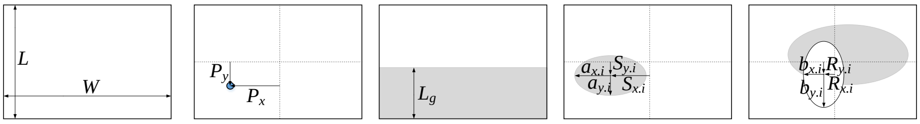

(a) (b) (c) (d) €

Fig. 1. Antenna parameterization building blocks: (a) substrate, (b) discrete port, (c) ground plane, (d) ith elliptical patch ($i = 1, \ldots, N_P$), (e) ith elliptical gap ($i = 1, \ldots, N_G$).

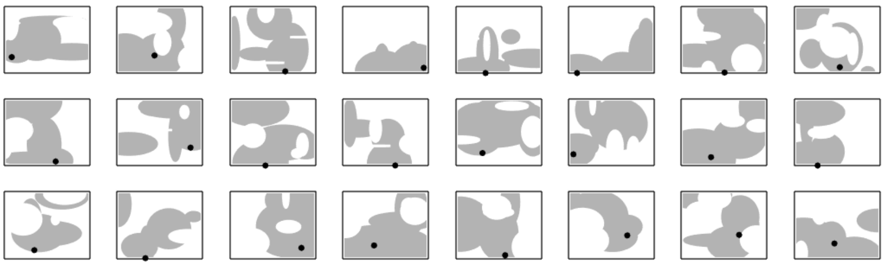

Fig. 2. Parameterization flexibility demonstrated through randomly generated architectures for $N_P = 5$ and $N_G = 3$. Front-side metallization marked gray; discrete port marked as a black dot.

ICCS Camera Ready Version 2025
To cite this paper please use the final published version:
DOI: 10.1007/978-3-031-97557-8_26

2.2 Computational Model

In this research, CST Microwave Studio [25] is utilized to implement and simulate the antenna's computational model. The template CST project incorporates ten and six patches and gaps, respectively, which is sufficient for real-world applications. When evaluating the device, the parameter vector $\boldsymbol{x}$ is recalculated into absolute dimensions and the excessive metal parts are trimmed to the substrate. The EM analysis is executed in a batch mode. Using a Visual Basic script, the template project is updated with the current antenna dimensions. The underlying programming environment for the presented framework is Matlab. Communication with CST is arranged using a custom-developed Matlab-CST interface, which also performs post-processing of the results exported upon accomplishing EM simulation. The operating flow of the process has been shown in Fig. 3.

2.3 Antenna Development

The design task considered here is a realization of multi-band antennas to ensure acceptable impedance matching, i.e., maintaining $|S_{11}| \leq -10$ dB over the frequencies. Let $F = [f_1 - B_1/2, f_1 + B_1/2] \cup [f_2 - B_2/2, f_2 + B_2/2] \cup \ldots \cup [f_K - B_K/2, f_K + B_K/2]$, denote target operating bands, where f_k and B_k are the center frequencies and the respective bandwidths. In rigorous terms, the objective is to solve the

$$\boldsymbol{x}^* = \arg\min_{\boldsymbol{x} \in X} U(\boldsymbol{x}) \tag{1}$$

where the cost function is given as

$$U(\boldsymbol{x}) = \max_{f \in F} \{ | S_{11}(\boldsymbol{x}, f) | \} \tag{2}$$

in which $|S_{11}(\boldsymbol{x},f)|$ is the modulus of the reflection coefficient at design $\boldsymbol{x}$ and frequency f. The design space is a box-constrained domain with lower/upper bounds imposed on antenna parameters (cf. Fig. 1). Note that mixing discrete and continuous parameters allows us to efficiently control the antenna's architecture and its specific dimensions. It is also possible to impose additional conditions, e.g., concerning the maximum antenna size, requirement for minimum gain, etc.). These scenarios will be considered elsewhere.

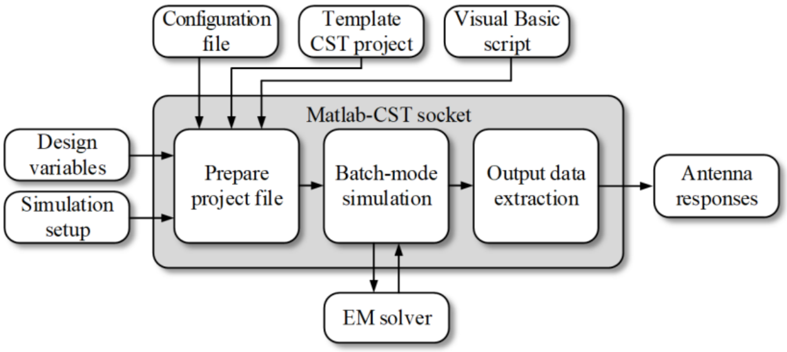

Fig. 3. Antenna's computational model. The EM model template uses decision variables (vector $\boldsymbol{x}$) and simulation setup to render the project file. Following the analysis, antenna responses are extracted from the EM data.

ICCS Camera Ready Version 2025
To cite this paper please use the final published version:
DOI: 10.1007/978-3-031-97557-8_26

In algorithmic terms, problem (1) is solved in two stages. The first is a global search process realized using a floating-point evolutionary algorithm incorporating elitism and adaptive mutation rate, which improves the exploitation capability of the procedure when close to convergence, see Fig. 4. At this stage, the antenna topology is decided upon along with a rough adjustment of its dimensions. The second stage is local tuning, which is executed with the trust-region (TR) gradient-based algorithm [27] with antenna response sensitivity computed using finite differentiation (FD) [28]. The algorithm's outline is shown in Fig. 5. At this stage, the antenna's topology has already been established, and only its dimensions are adjusted to boost the device's performance regarding the merit function (2). The TR algorithm produces approximate solutions using predictions from a linear model of antenna outputs (cf. (6)). The problem (6) is solved using the Sequential Quadratic Approximation (SQP) routine [29] available in Matlab [30]. Using FD entails the cost of n + 1 EM analyzes per iteration, where n is the overall number of decision variables. These expenses are reduced by eliminating the variables that have minor effects on antenna characteristics upon initial pre-screening. Also, the global search stage employs coarse-discretization EM analysis, which further improves computational efficiency. The accurate (high-fidelity) model is only used for final tuning.

The algorithm's structure is similar to evolutionary procedures (e.g., [26]). Main features:

- Generational model (a new population entirely replaces the previous one);
- Population size N = 20;
- Selection scheme: binary tournament;
- Elitism: a single best individual is stored and inserted to the next population;
- Recombination: a mixture of intermediate and arithmetic crossover:
  - Parent individuals: $\boldsymbol{x} = [x_1 \dots x_n]^T$ and $\boldsymbol{y} = [y_1 \dots y_n]^T$; offspring: $\boldsymbol{z} = [z_1 \dots z_n]^T$;
  - Intermediate crossover: $z_i = ax_i + (1-a)y_i$ with $0 \le a \le 1$ (a selected randomly);
  - Arithmetic crossover: $\boldsymbol{z} = a\boldsymbol{x} + (1 - a)\boldsymbol{y}$ with $0 \le a \le 1$ (a selected randomly).
  - Crossover probability is set to $p_m = 0.8$;
- Mutation: Random mutation with nonuniform probability distribution. It is applied individually to each parameter vector component so that $x_i \to x_i' + \Delta x_i$, where Δx_i is a random deviation defined as

$$\Delta x_i = \begin{cases} (x_{i.\max} - x_i)\cdot(2(r-0.5))^{\beta} & \text{if } r > 0.5 \\ (x_{i.\min} - x_i)\cdot(2(0.5-r))^{\beta} & \text{otherwise} \end{cases} \tag{3}$$

  where $r \in [0,1]$ is a random number and $\beta = 3$;
- Algorithm termination: maximum number of $N_i = 100$;
- Adaptive adjustment of mutation rate p_m. Let P_D be a population diversity defined as

$$P_D = \frac{1}{n}\sum_{k=1}^{n} std\left(\left[x_{1.k}\ x_{2.k}\ \dots\ x_{N.k}\right]\right) \tag{4}$$

  where $\boldsymbol{x}^j = [x_{j.1} \dots x_{j.n}]^T$ is jth member of the population, and $x_{j.k}$ is its kth entry. The mutation rate $p_m^{(i+1)}$ for iteration i of the algorithm is set as follows (initial value $p_m^{(0)} = 0.2$): if $i < N_i/2$ then adjust p_m based on P_D, else $p_m^{(i+1)} = p_m^{(Ni/2)}[2(N_i-1)/N_i]^2$. Adaptation for P_D: if $P_D < P_{D\min}$ then $p_m^{(i+1)} = p_m^{(i)}m_{incr}$, elseif $P_D > P_{D\max}$ then $p_m^{(i+1)} = p_m^{(i)}/m_{decr}$.

<u>Remark</u>: Setup: $P_{D\min} = 0.05$, $P_{D\max} = 0.1$, and $m_{incr} = 1.3$, $m_{decr} = 1.2$. $P_{D\min}$ and $P_{D\min}$ are set considering antenna parameters are relative (i.e., between zero and unity).

Fig. 4. The global search stage of antenna development: evolutionary algorithm.

ICCS Camera Ready Version 2025
To cite this paper please use the final published version:
DOI: 10.1007/978-3-031-97557-8_26

2.4 Design Framework

The operation of the suggested unsupervised antenna design methodology is illustrated in Fig. 6. The process is purely specification-driven and does not involve any human-expert interaction. The input data consists of the intended substrate parameters (thickness, relative permittivity), the size (if not optimized), and, most importantly, the target operating frequency ranges. The number of unit cells, N_P and N_G, can be decided upon beforehand. The antenna topology evolves during the global search stage. It is further refined through final tuning.

3 Results

This part of the work showcases the performance of the unsupervised design procedure. It is used to develop several antenna structures based on different design specifications concerning the target operating frequency bands. The results are encapsulated in Sections 3.1 through 3.4, whereas Section 3.5 discusses the findings. Furthermore, Section 3.6 provides experimental validation of the selected designs.

Final tuning task:

$$\boldsymbol{x}^* = \arg\min_{\boldsymbol{x}\in X} U(\boldsymbol{x}) \tag{5}$$

TR algorithm: the procedure generates a sequence $\boldsymbol{x}^{(i)}$, $i = 0, 1, 2, \ldots$ as

$$\boldsymbol{x}^{(i+1)} = \arg\min_{\boldsymbol{x};\, ||\boldsymbol{x}-\boldsymbol{x}^{(i)}|| \le d^{(i)}} U_L(\boldsymbol{x}) \tag{6}$$

The merit function U_L is the same as U but with S_{11} evaluated using a linear model:

$$S_{11L}^{(i)}(\boldsymbol{x},f) = S_{11L}^{(i)}(\boldsymbol{x}^{(i)},f) + \boldsymbol{G}_{11}(\boldsymbol{x}^{(i)},f)\cdot(\boldsymbol{x}-\boldsymbol{x}^{(i)}) \tag{7}$$

Here, $\boldsymbol{G}_{11}(\boldsymbol{x},f)$ is the gradient of $S_{11}(\boldsymbol{x},f)$ at $\boldsymbol{x}$ and frequency f, computed using FD [28].

Other operating details:

- $\boldsymbol{x}^{(i+1)}$ is accepted if the gain ratio $r = [U(\boldsymbol{x}^{(i+1)}) - U(\boldsymbol{x}^{(i)})]/[U_L(\boldsymbol{x}^{(i+1)}) - U_L(\boldsymbol{x}^{(i)})] > 0$ (i.e., EM-simulated cost function is improved); otherwise, the iteration is repeated with reduced TR size;
- The trust region size $d^{(i)}$ is adaptively adjusted based on r; $d^{(i+1)} = d^{(i)}m_{incr}$ if $r > r_{incr}$, and $d^{(i+1)} = d^{(i)}/m_{decr}$ if $r < r_{decr}$; the control parameters are $r_{incr} = 0.75$, $r_{decr} = 0.25$, $m_{incr} = 1.5$, $m_{decr} = 2$ [27];
- Termination criteria: convergence in argument ($||\boldsymbol{x}^{(i+1)} - \boldsymbol{x}^{(i)}|| < \varepsilon$) or sufficient reduction of the TR size ($d^{(i)} \le \varepsilon$); the termination threshold is set to $\varepsilon = 10^{-3}$.

Fig. 5. Final tuning using the TR algorithm.

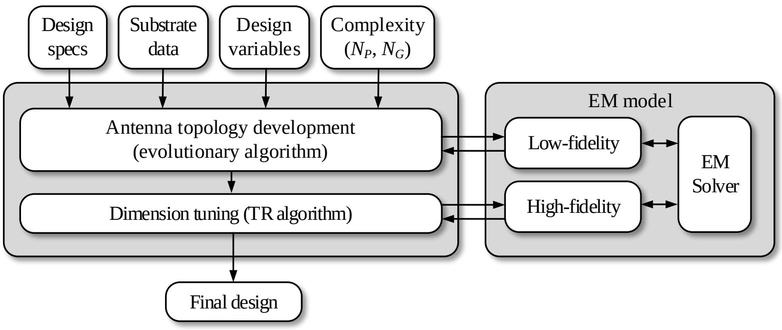

Fig. 6. Proposed design framework: the flow diagram.

ICCS Camera Ready Version 2025
To cite this paper please use the final published version:
DOI: 10.1007/978-3-031-97557-8_26

All designs are realized on FR-4 dielectric substrate ($\varepsilon_r = 4.4$, $h = 1.0$ mm) or the size $W = 30$ mm and $L = 20$ mm (except Example II, which uses $W = 25$ mm and $L = 15$ mm). The model complexity is $N_P = 5$, $N_G = 3$. The evolutionary algorithm runs for 100 iterations with a population size of 20. The global search stage uses a low-fidelity EM model (simulation time ~20 seconds). The final tuning is based on the high-fidelity model (simulation time ~60 seconds).

3.1 Example I

The first case is a single-band antenna operating from 5 GHz to 6 GHz. The structure generated by the suggested framework, the impedance matching characteristic, and the history of the development process can be found in Fig. 7. Note that global search has produced a satisfactory outcome. It is further improved through local tuning. It should be stressed that the entire procedure is purely specification-based. No human expert is necessary whatsoever.

3.2 Example II

The next validation case is a compact ultra-wideband (UWB) antenna. The target frequency range is from 3.1 GHz to 10.6 GHz. The antenna substrate is diminished to only 15 mm × 25 mm compared to the remaining test cases. The obtained architecture and the history of the development process can be found in Fig. 8.

3.3 Example III

The third case is a dual-band antenna. The target ranges are from 2.4 GHz to 2.5 GHz (lower band) and from 5.2 GHz to 5.4 GHz (upper band). As indicated in Fig. 9, the proposed framework yields a design fulfilling the specifications already at the geometry evolution stage. Local tuning only slightly improves the impedance matching.

3.4 Example IV

The last test case is a triple-band antenna. The target frequency ranges are from 2.4 GHz to 2.5 GHz, 5.2 GHz to 5.4 GHz, and 7.5 GHz to 8.0 GHz. Figure 10 shows the antenna structure found by the presented framework and the development history. As observed, the specifications for this challenging example are met for the lower and middle bands. Only a slight violation is observed in the upper band.

3.5 Discussion

The data showcased in Sections 3.1 through 3.4 underscores the capability of the presented framework to successfully develop antenna structures for diverse performance specifications. The design process is unsupervised, with the only input data being the intended number of operating bands and the target frequency ranges. The topologies produced by the proposed algorithm are highly unconventional yet evolved to adequately utilize all antenna components, which is illustrated using surface current distributions shown in Fig. 11.

ICCS Camera Ready Version 2025
To cite this paper please use the final published version:
DOI: 10.1007/978-3-031-97557-8_26

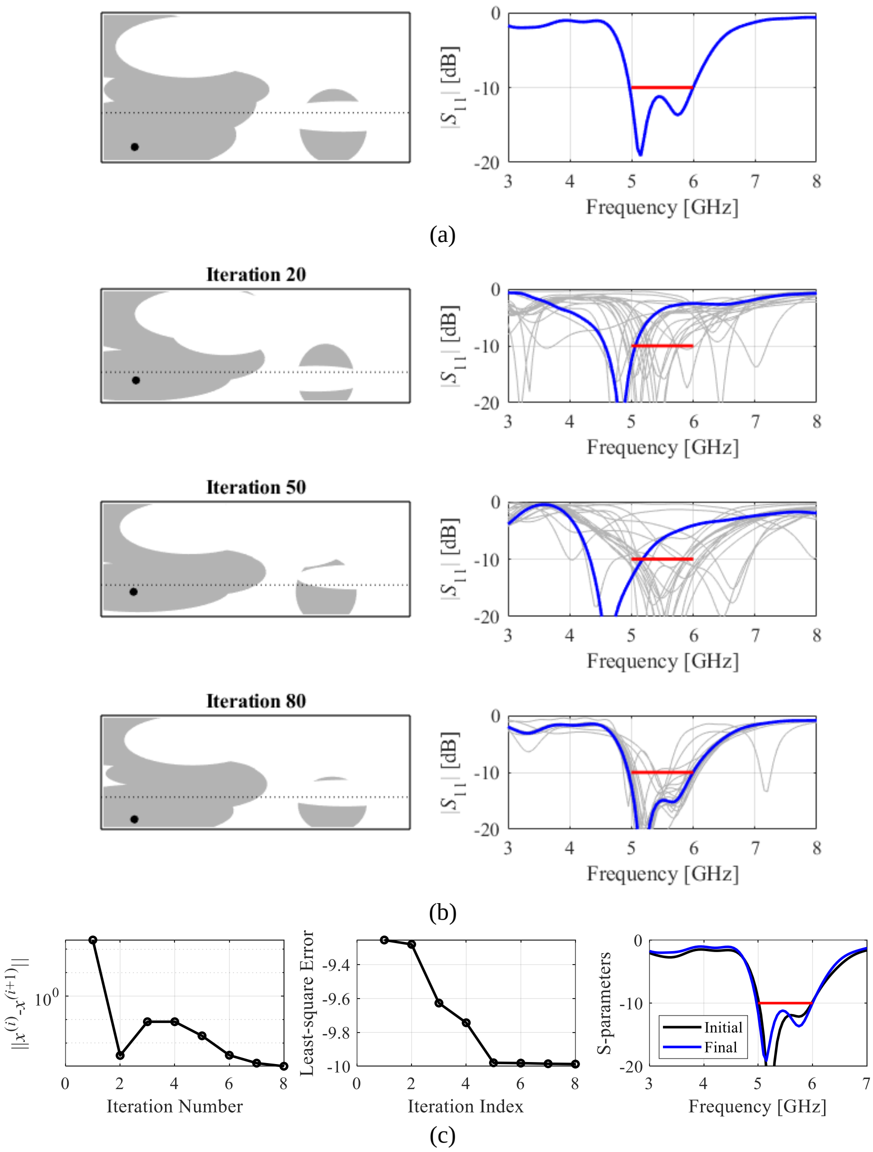

Fig. 7. Example I: target frequency range from 5.0 GHz to 6.0 GHz: (a) final topology (ground plane ····) and $|S_{11}|$ characteristic; (b) topology evolution (the best architecture marked using the blue line; antenna outputs at the current population marked using gray lines); (c) local tuning (convergence plot, merit function vs. iteration index, and initial/final reflection response).

ICCS Camera Ready Version 2025
To cite this paper please use the final published version:
DOI: 10.1007/978-3-031-97557-8_26

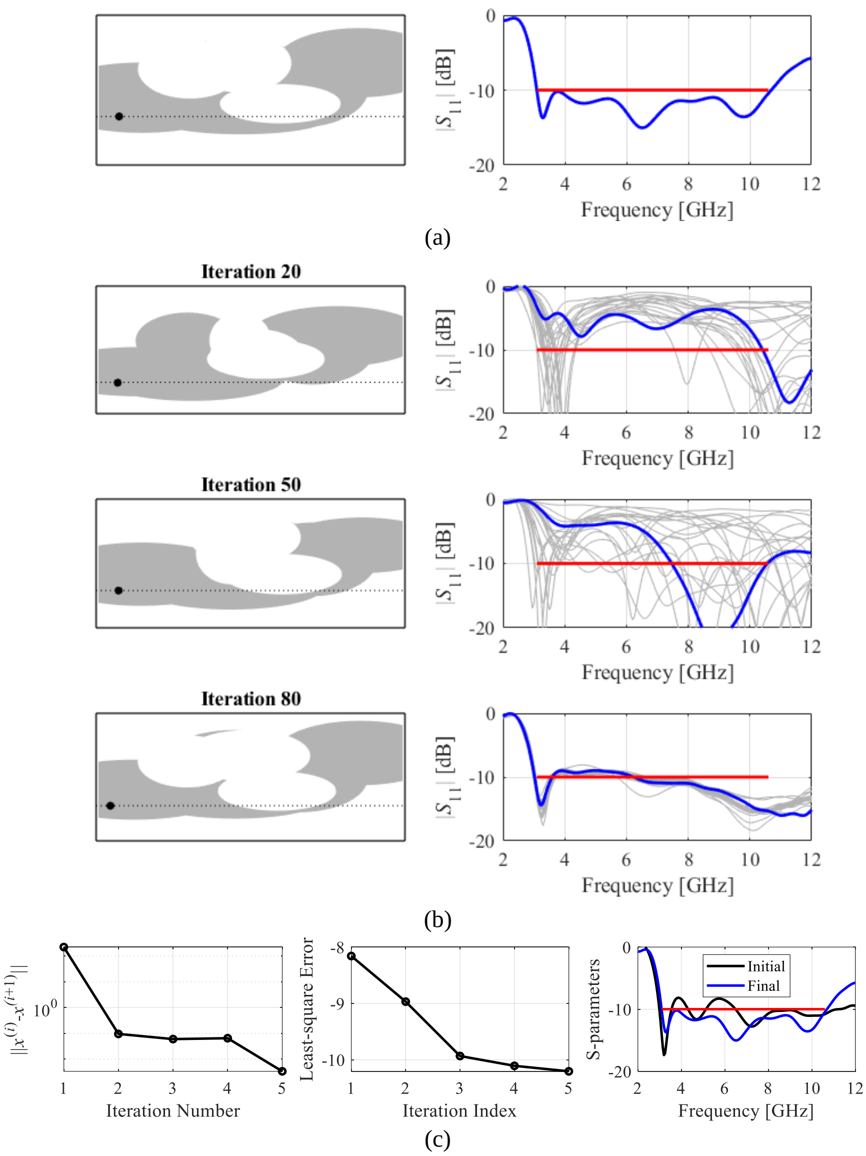

Fig. 8. Example II: an ultra-wideband antenna; target frequency range from 3.1 GHz to 10.6 GHz: (a) final topology (ground plane ····) and $|S_{11}|$ characteristic; (b) topology evolution (the best architecture marked using the blue line; antenna outputs at the current population marked using gray lines); (c) local tuning (convergence plot, merit function vs. iteration index, and initial/final reflection response).

ICCS Camera Ready Version 2025
To cite this paper please use the final published version:
DOI: 10.1007/978-3-031-97557-8_26

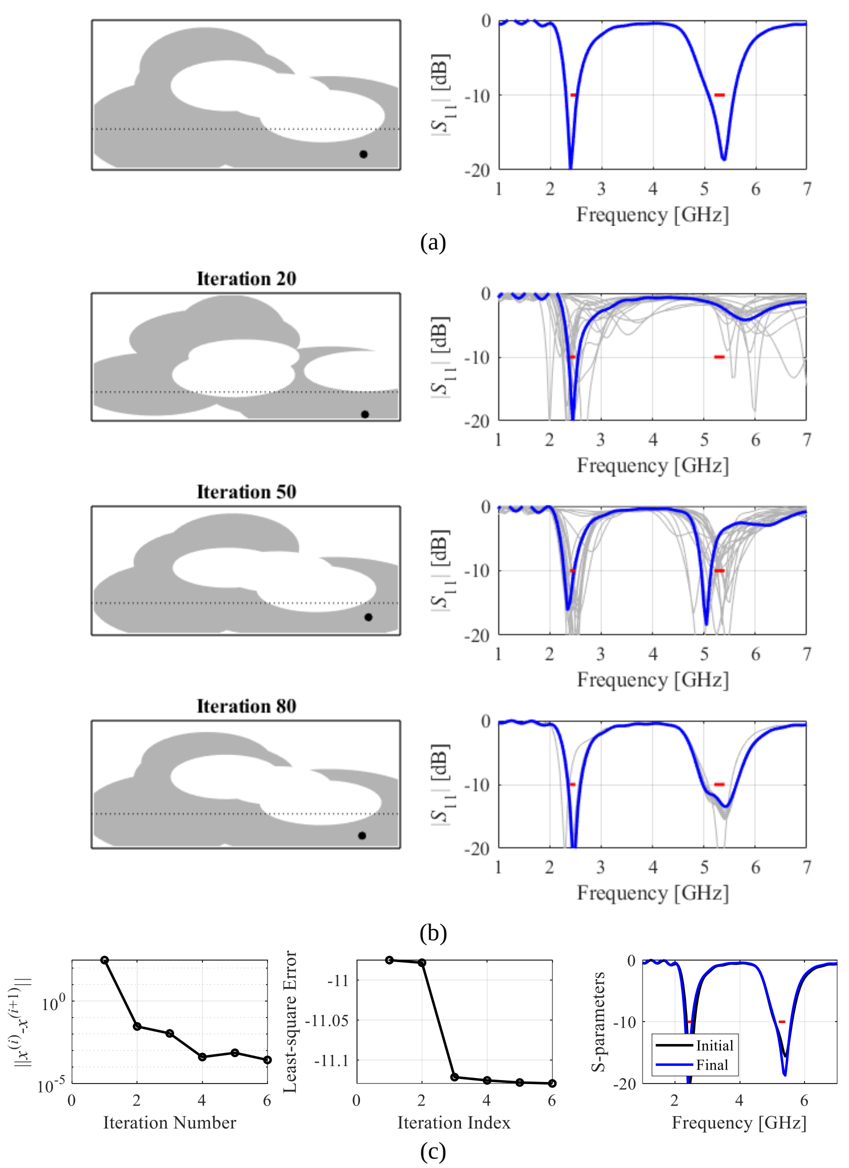

Fig. 9. Example III: target frequency ranges from 2.4 GHz to 2.5 GHz and from 5.2 GHz to 5.4 GHz: (a) final topology (ground plane ····) and $|S_{11}|$ characteristic; (b) topology evolution (the best architecture marked using the blue line; antenna outputs at the current population marked using gray lines); (c) local tuning (convergence plot, merit function vs. iteration index, and initial/final reflection response).

ICCS Camera Ready Version 2025
To cite this paper please use the final published version:
DOI: 10.1007/978-3-031-97557-8_26

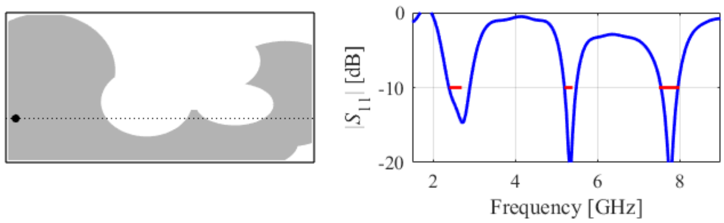

(a)

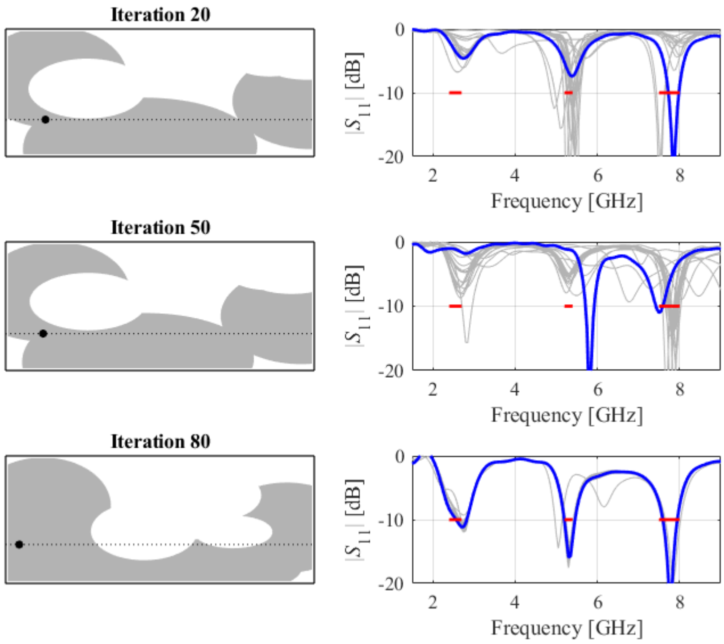

(b)

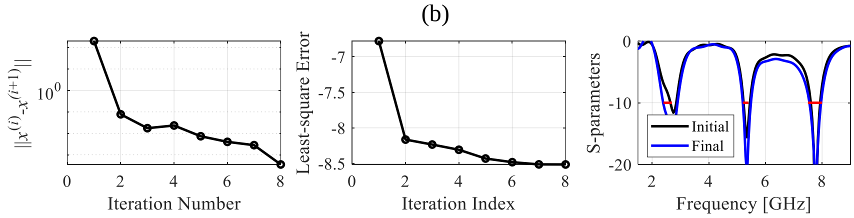

(c)

Fig. 10. Example IV: target frequencies from 2.4 GHz to 2.5 GHz, 5.2 GHz to 5.4 GHz, and 7.5 GHz to 8.0 GHz: (a) final topology (ground plane ····) and $|S_{11}|$ characteristic; (b) topology evolution (the best architecture marked using the blue line; antenna outputs at the current population marked using gray lines); (c) local tuning (convergence plot, merit function vs. iteration index, and initial/final reflection response).

It is also important to emphasize that all considered antennas were obtained using identical algorithm setups and at an acceptable computational cost from a practical engineering perspective (about fifteen hours of CPU time).

ICCS Camera Ready Version 2025
To cite this paper please use the final published version:
DOI: 10.1007/978-3-031-97557-8_26

3.6 Experimental Validation

The antennas developed in Sections 3.2 and 3.4 (Examples II and IV) were manufactured and experimentally validated for additional demonstration. The results are shown in Figs. 12 and 13. As observed, the alignment between EM simulations and measurements is satisfactory. Minor discrepancies are due to fabrication tolerances and assembly inaccuracies.

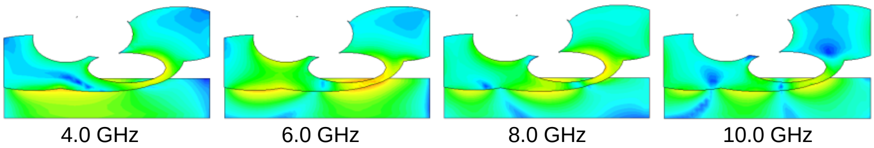

(a)

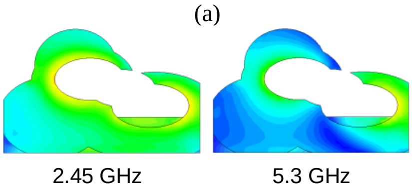

(b)

Fig. 11. Surface currents for (a) Example II, (b) Example III. Observe the use of the diverse antenna components at diverse frequencies (increasing current density corresponds to the transition from blue to red through green and yellow color). This demonstrates the importance of each building block employed to assemble the antenna structures.

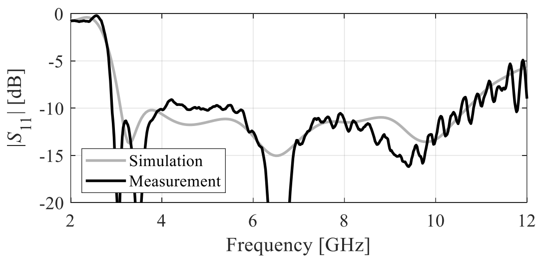

(a) (b)

Fig. 12. Example II: (a) prototype, (b) simulated and measured $|S_{11}|$.

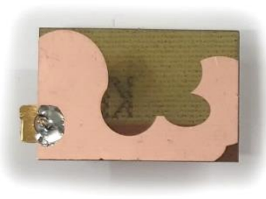

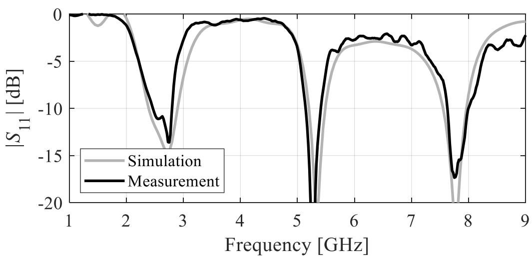

(a) (b)

Fig. 13. Example IV: (a) prototype, (b) simulated and measured $|S_{11}|$.

DOI: 10.1007/978-3-031-97557-8_26

4 Conclusion

This work introduces an innovative methodology for an automated design of antennas, which employs computational intelligence and numerical optimization methods. Capitalizing on flexible parameterization and simultaneous adjustment of discrete and continuous parameters determining the antenna architecture and its dimensions, the proposed technique can produce high-quality designs in a purely specification-driven manner. This has been extensively demonstrated using several examples of single-, dual-, triple-, and broadband devices and further corroborated through experimental validation of selected designs. The developed method can be viewed as an attractive approach to the automated development of unconventional antenna structures for demanding applications using reasonable computational resources.

Acknowledgment

The authors thank Dassault Systemes, France, for making CST Microwave Studio available. This work is partially supported by the Icelandic Centre for Research (RANNIS) Grant 239858 and by the National Science Centre of Poland Grant 2020/37/B/ST7/01448.

References

1. Ullah, U., Al-Hasan, M., Koziel, S., Ben Mabrouk I. Circular polarization diversity implementation for correlation reduction in wideband low-cost multiple-input-multiple-output antenna. IEEE Access, **8**, 95585–95593 (2020)
2. Zeng, Y., Qing, X., Chia M.Y.W. A wideband circularly polarized antenna with a nonuniform metasurface designed via multiobjective Bayesian optimization. IEEE Ant. Wireless Propag. Lett., **23**, 1739–1743 (2024).
3. Lucchini, F., Torchio, R., Bettini, P., Dughiero F. TopIE: an integral equation tool for topology optimization in electromagnetics. IEEE Trans. Ant. Propag., **72**, 683–692 (2024)
4. Koziel, S., Pietrenko-Dabrowska, A., Global EM-driven optimization of multi-band antennas using knowledge-based inverse response-feature surrogates. Knowledge Based Systems. **227**, paper no. 107189 (2021)
5. Tan, J., Shao, Y., Zhang, J., Zhang J. Efficient antenna modeling and optimization using multifidelity stacked neural network. IEEE Trans. Ant. Propag. **72**, 4658–4663 (2024)
6. Koziel, S., Pietrenko-Dabrowska, A., Recent advances in accelerated multi-objective design of high-frequency structures using knowledge-based constrained modeling approach. Knowledge Based Systems. **214**, paper no. 106726 (2021)
7. Li, J., Sun, G., Duan, L., Wu Q. Multi-objective optimization for UAV swarm-assisted IoT with virtual antenna arrays. IEEE Trans. Mobile Comp. **23**, 4890–4907 (2024)
8. Zhang, Z., Chen, H.C., Cheng Q.S. Surrogate-assisted quasi-newton enhanced global optimization of antennas based on a heuristic hypersphere sampling. IEEE Trans. Ant. Propag., **69**, 2993–2998 (2021)
9. He, Y., Huang, J., Li, W., Zhang, L., Wong, S.W., Chen Z.N. Hybrid method of artificial neural network and simulated annealing algorithm for optimizing wideband patch antennas. IEEE Trans. Antennas Propag., **72**, 944–949 (2024)

ICCS Camera Ready Version 2025
To cite this paper please use the final published version:
DOI: 10.1007/978-3-031-97557-8_26

10. Liu, Y., Chen, P., Tian, J., Xiao, J., Noghanian, S., Ye Q. Hybrid ANN-GA optimization method for minimizing the coupling in MIMO antennas. AEU – Int. J. Electronics Comm. **175**, paper no. 155068 (2024)
11. Yasmeen, K., Mishra, K.V., Subramanyam, A.V., Ram S.S. Circularly polarized Fabry–Pérot cavity sensing antenna design using generative model. IEEE Sensors Lett., **7**, 1–4 (2023)
12. Pietrenko-Dabrowska, A., Koziel, S., Response feature technology for high-frequency electronics. Optimization, modeling, and design automation. Springer, New York, 2023.
13. Koziel, S., Pietrenko-Dabrowska, A., Fast EM-driven nature-inspired optimization of antenna input characteristics using response features and variable-resolution simulation models. Sc. Rep. **14**, paper no. 10081 (2024)
14. Sarker, N., Podder, P., Mondal, M.R.H., Shafin, S.S., Kamruzzaman J. Applications of machine learning and deep learning in antenna design, optimization, and selection: a review. IEEE Access, **11**, 103890–103915 (2023)
15. Zhong, Y., Renner, P., Dou, W., Ye, G., Zhu, J., Liu „A machine learning generative method for automating antenna design Q.H. . IEEE Trans. Ant. Propag., **68**, 6858–6866 (2020)
16. Liu, P., Chen, L., Chen Z.N. Prior-knowledge-guided deep-learning-enabled synthesis for broadband and large phase shift range metacells in metalens antenna. IEEE Trans. Ant. Propag., 70, 5024–5034 (2022)
17. Jiang, F., Chiu, C.-Y., Shen, S., Cheng, Q.S., Murch R. Pixel antenna optimization using N-port characteristic mode analysis. IEEE Trans. Ant. Propag., **68**, 3336–3347 (2020)
18. Chen, Y.-S., Chiu, Y.-H., Application of multiobjective topology optimization to miniature ultrawideband antennas with enhanced pulse preservation. IEEE Ant. Wireless Propag. Lett., **15**, 842–845 (2016)
19. Jiang, F., Shen, S., Chiu, C.Y., Zhang, Z., Zhang, Y., Cheng, Q.S., Murch, R. Pixel antenna optimization based on perturbation sensitivity analysis. IEEE Trans. Ant. Propag., **70** (1), 472–486 (2022)
20. Zheng, W., Li, H., Designing antennas with quasi-isotropic radiation patterns using pixel structures. IEEE Trans. Ant. Propag., **71**, 7813–7823 (2023)
21. Zhu, S.-H., Yang, X.-S., Wang, J., Wang B.-Z. Design of MIMO antenna isolation structure based on a hybrid topology optimization method. IEEE Trans. Ant. Propag., **67**, 6298–6307 (2019)
22. Wang, J., Yang, X.-S., Ding, X., Wang B.-Z. Topology optimization of conical-beam antennas exploiting rotational symmetry. IEEE Trans. Ant. Propag., **66**, 2254–2261 (2018)
23. Tucek, J., Capek, M., Jelinek, L., Sigmund O. Density-based topology optimization in method of moments: Q-factor minimization. IEEE Trans. Ant. Propag., **71**, 9738–9751 (2023)
24. Wang, L.L., Yang, X.S., Ma C.J. An efficient gradient-based hybrid parameter-topology optimization for antenna design. IEEE Trans. Ant. Propag., **71**, 9477–9486 (2023)
25. CST Microwave Studio, ver. 2023, Dassault Systemes, France (2023)
26. Michalewicz, Z., Genetic algorithms + data structures = evolution programs. Springer, New York (1996)
27. Conn, A.R., Gould, N.I.M., Toint, P.L. Trust Region Methods, MPS-SIAM Series on Optimization (2000)
28. Levy, H., Lessman, F.. Finite Difference Equations, Dover Publications Inc., New York (1992)
29. Nocedal, J., Wright, S.J. Numerical Optimization, 2nd Ed., Springer, New York, (2006)
30. Matlab, ver. 2023a, MathWorks Inc., Natick, MA, USA (2023)

ICCS Camera Ready Version 2025
To cite this paper please use the final published version:
DOI: 10.1007/978-3-031-97557-8_26